Korean J. of Chem. Eng., 3(1) (1986) 7-13

PARTITION CHARACTERISTICS OF CLOSE-BOILING COMPONENTS IN A CHROMATOGRAPHIC COLUMN

Kyung Ho ROW and Won Kook LEE*

Department of Chemical Engineering, Korea Advanced Institute of Science and Technology P.O. Box 131 Dongdaemoon, Seoul 131, Korea

(Received 7 May 1985 • accepted 2 October 1985)

Abstract—Partition characteristics of three close-boiling components (dichloromethane, diethylether, and dimethoxymethane) were investigated with dinonylphthalate-coated Chromosorb A and helium as the carrier. The outlet stream from the chromatographic column was monitored continuously. Partition coefficients were experimentally determined at various column temperatures for the three components. With the assumption of uniform film thickness, two parameters were estimated by Fourier analysis of the response curves. The Peclet number for particle was expressed in terms of the Reynolds number and the Schmidt number as:

$$\frac{1}{Pe,p}=\frac{0.87}{Re\cdot Sc}+0.5$$

Intraparticle diffusion coefficient of each component was also determined in the form of the dimensionless group, P_i.

The theoretical response curve in time domain was in good agreement with the observed one. From the sensitivity analysis, it is concluded that the liquid film resistance was small and the diffusion in the liquid phase was not a rate-determining step.

INTRODUCTION

Among a variety of procedures for accurate and fast separation of mixtures, one of the most powerful and versatile separation processes is chromatography. [1].

In a gas-liquid chromatography, components are separated by different solubilities in the non-volatile liquid phase [2]. In spite of a large number of works related to separation by adsorption characteristics [3, 4], those by partition are relatively scarce [5]. The main advantages of this system in comparison to adsorption are easier desorption of the partitioned products and wider application [6].

The distribution of the liquid phase on the porous solid support is not easy to describe, but the concept of uniform film thickness is reasonably acceptable. Such model equations are usually based on the assumption of linear isotherm, and the resulting linear partial differential equations can be solved in the Laplace domain.

The purpose of this study is to investigate the effect of the parameters used in the model under the assumption of uniform film thickness by the frequency domain. Materials used in the present work were three close-boiling components which are dichloromethane, diethylether, and dimethoxymethane.

*To whom all correspondence should be addressed.

UNIFORM FILM THICKNESS MODEL

Transient material balances for the solute with uniform film thickness of the liquid phase were given by Alkharasani and McCoy [7]. The equations are

$$\frac{\partial C}{\partial t}+u\frac{\partial C}{\partial z}=\frac{D_o}{\varepsilon}\frac{\partial^2 C}{\partial z^2}-\frac{3}{r_P}\frac{1-\varepsilon}{\varepsilon}D_e\frac{\partial q}{\partial r}\Big|_{r=r_P} \quad (1)$$

for the mobile phase,

$$\varepsilon_s\frac{\partial C_s}{\partial t}=D_e\frac{1}{r^2}\frac{\partial}{\partial r}\left(r^2\frac{\partial C_s}{\partial r}\right)-A_P k_g\left(C_s-\frac{C_l|_{x=\sigma}}{K}\right) \quad (2)$$

for the intraparticle phase, and

$$\frac{\partial C_l}{\partial t}=D_l\frac{\partial^2 C_l}{\partial x^2} \quad (3)$$

for the liquid phase.

The initial and boundary conditions are:

$$C=C_s=C_l=0 \quad (\text{for } t=0,\ z>0) \quad (4)$$

$$C=\delta(t) \quad (\text{for } t>0,\ z=0) \quad (5)$$

$$C=\text{finite} \quad (\text{for } t>0,\ z\to\infty) \quad (6)$$

$$C_s = \text{finite} \qquad (\text{for } t>0,\ r=0) \tag{7}$$

$$\frac{\partial C_t}{\partial x} = 0 \qquad (\text{for } t>0,\ x=0) \tag{8}$$

$$D_e \frac{\partial C_s}{\partial r} = k_f (C - C_s) \qquad (\text{for } t>0,\ r=r_p) \tag{9}$$

$$D_t \frac{\partial C_t}{\partial x} = k_g \left(C_s - \frac{C_t}{K}\right) \qquad (\text{for } t>0,\ x=\delta) \tag{10}$$

The following dimensionless groups are introduced.

$$P_e = \frac{uL\varepsilon}{D_o},\quad P_t = \frac{\varepsilon_s r_p^2 u}{D_e L},\quad P_t = \frac{\delta^2 L}{D_t L}$$

$$S_t = 3\frac{1-\varepsilon}{\varepsilon}\frac{k_f L}{r_p u},\quad S_t M = \frac{A_p k_g L}{\varepsilon_s u}$$

$$B_i = \frac{k_f r_p}{D_e},\quad B_t M = \frac{k_g \delta}{D_t},\quad \eta = \frac{C}{C_o},\quad \theta = \frac{ut}{L}.$$

The solution of Eq. (1) to Eq. (10) in the Laplace domain with the dimensionless groups is

$$\bar{\eta} = \frac{1}{s}\exp\left\{\frac{1}{2}(P_e - \sqrt{P_e^2 + 4\lambda_1})\right\} \tag{11}$$

at the bed exit, z=L, where

$$\lambda_1 = \{s + S_t(1-\lambda_2 \sinh \lambda_3)\} P_e \tag{12}$$

$$\lambda_2 = B_t / \{\lambda_3 \cosh \lambda_3 - \sinh \lambda_3 + B_i \sinh \lambda_3\} \tag{13}$$

$$\lambda_3 = -P_t(s + S_t M) - \frac{B_t M\ S_t M\ P_t \cosh(\sqrt{P_t s})}{B_t M \cosh\sqrt{P_t s} + K\sqrt{P_t s}\ \sinh\sqrt{P_t s}}\Big\}^{\frac{1}{2}} \tag{14}$$

The solution in the frequency domain is obtained by substituting $s=j\omega$ in the s-domain, and the amplitude ratio and the phase of the Fourier transformed equation can be computed.

The objective function, ψ, is defined as follows:

$$\psi = \int_0^\infty \{f_o(t) - f_p(t)\}^2 dt \tag{15}$$

From the Parseval theorem, we find that

$$\psi = \frac{1}{\pi}\int_0^\pi |F_o(j\omega) - F_p(j\omega)|\, d\omega \tag{16}$$

Thus parameters can be estimated from the minimization of ψ.

MATERIALS AND METHOD

Close-Boiling Components

Dichloromethane (DCM), diethylether (DEE), and dimethoxymethane (DMM) were used as feed components. Their boiling points are 39.8°C, 34.6°C, and 41.5°C, respectively.

Packing Materials

The packing used in this work was Chromosorb A (Alltech Associates, Illinois, U.S.A), and this was selected because it is used for large-scale chromatographic separation.

The Chromosorb A of three particle sizes (60/80, 45/60, and 20/30 mesh) were used, and the average particle sizes were determined by screen analysis.

The ratio of the liquid phase to the solid particle was 0.25 by weight for all particle sizes. The interparticle porosity was assumed to be 0.41 [8], and the intraparticle porosities of 25%-coated porous particle were measured by a mercury porosimeter at atmospheric pressure for three particle sizes. Typical properties of Chromosorb A are given in Table 1.

Table 1. Typical properties of Chromosorb A.

	20/30mesh	45/60mesh	60/80mesh
r_p (cm)	0.03125	0.01360	0.00996
ϵ_s'	0.66	0.78	0.78
ϵ_s	0.50	0.62	0.62
A_p (cm^2/cm^3) [9]	13,000		
A_s (g/cm^3) [9]	27,000		
true density (g/cm^3)	2.3		

Method

The columns were glass tubes tapered at the bottom sides whose inner diameters were fixed at 1.0 cm with lengths of 25, 50, and 75cm. The packed bed in the column was supported by a thin pad of fine glass wool, and the columns were packed by using a vibrator. The column was covered with ceramics to keep the temperature constant.

A sample of 5μl volume was injected to the bottom of the column by a syringe. The feed was vaporized into a stream of helium before entering into the column. The outlet stream from the chromatographic column was monitored continuously.

Each curve from the chromatographic column was divided, and coordinates of those were read by an HP 9845 digitizer.

RESULTS AND DISCUSSION

Measurement of Partition Coefficient

The partition coefficient is usually defined by the ratio of the retention volume in the mobile phase to the quantity of the liquid phase [10]. Figure 1 indicates that retention volumes were independent of the concentration in the injected pulse. The retention volumes were experimentally obtained from a conventional gas chromatograph, and the partition coefficients could be obtained by measuring the quantity of the liquid phase [11].

The effect of the column temperature on the partition

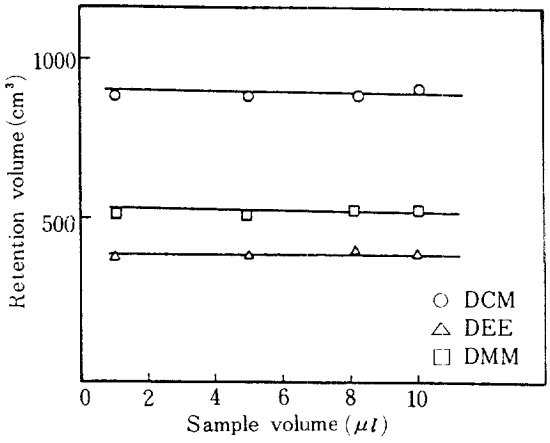

Fig. 1. Effect of sample volume on retention volume at 40℃,
(u_o=3.71cm/sec, 45/60mesh, L=50cm).

coefficient was correlated as [12].

$$K = K_o \exp(-\Delta H_s/RT) \quad (17)$$

where $-\Delta H_s$ (cal/gmol) = heat of solution
R (cal/gmol °K) = gas constant

Figure 2 shows the effect of the column temperature on the partition coefficient. From the slope of each straight line in the figure, the heat of solution could be obtained. K_0 and $-\Delta H_S$ of each component are listed in Table 2.

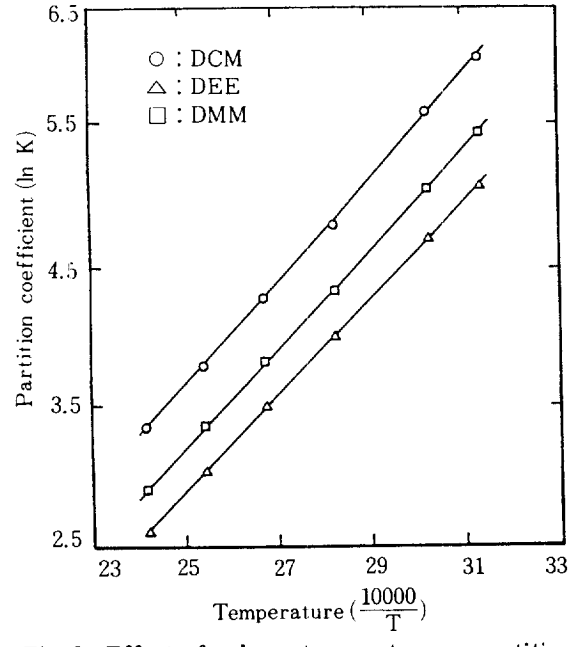

Fig. 2. Effect of column temperature on partition coefficient.

Table 2. K_o and $-\Delta H_S$ used in Eq. (17).

	K_o	$-\Delta H_S$ (cal/gmol)
DCM	0.00298	7043.9
DEE	0.00167	6875.0
DMM	0.00231	6894.9

Determination of Parameters used in the Model

The film thickness, δ, was obtained as 0.127 μm under the assumption of uniform distribution of the liquid phase on the porous solid support at 25% liquid loading [13]. Fixed parameters used in the uniform film thickness model are listed in Table 3.

Two adjustable parameters, η_{ext} and P_i were estimated by using Fourier analysis. Due to the nonlinearity of the expression, the parameters were determined by an optimization technique suggested by Marquart [18]. The axial dispersion coefficient in a packed column is expressed as a sum of the molecular diffusion and the eddy diffusion [19].

$$D_o = \eta_{ext} D_M + r_P u_o \quad (18)$$

Edwards [20] showed that molecular diffusion becomes important at Reynolds number smaller than 3×10^{-4} for liquids and 1.8 for gases. The effect of the superficial velocity of carrier may be significant because of its higher flow rate. It is possible to estimate the external tortuosity from the impulse injection test at different superficial velocities of carrier and particle sizes. After the axial dispersion coeffiecient was estimated, the Peclet number for particle ($Pe, p = \frac{2u_o r_P}{D_o}$) was expressed in terms of the Reynolds number (Fig. 5) as follows:

$$\frac{1}{Pe, p} = \frac{0.87}{Re \cdot Sc} + 0.5, \quad (19)$$

where $Re = \frac{2r_P u_o \rho}{\mu_G}$ and $Sc = \frac{\mu_G}{\rho D_M}$.

Table 3. Fixed parameters used in this work.

δ (cm) [13]	$\delta = \frac{w_L}{\rho_L A_S w_S}$		
k_f (cm/sec) [14]	$k_f = \frac{D_M}{r_P}(1+0.725 R_e^{1/2} S_c^{1/3})$		
k_g (cm/sec) [15]	$k_g = \frac{D_M}{r_P}(12.5\frac{1-\varepsilon_S}{\varepsilon_S})$		
	DCM	DEE	DMM
D_M (cm^2/sec) [16]	0.488	0.410	0.441
D_i (cm^2/sec) [17]	1.28×10^{-6}	1.01×10^{-6}	1.12×10^{-6}
K	247.2	105.6	150.8

Table 4. Result from frequency domain analysis for DCM. (Adjustable parameters: η_{ext}, P_i)

L (cm)	particle size (r_P; cm)	u_o (cm/sec)	η_{ext}	P_i
75	45 / 60 mesh (0.0136)	7.73	1.26	0.0114
		4.08	0.70	0.0115
		2.43	0.45	0.0115
50	20 / 30 mesh (0.03125)	6.28	1.05	0.0114
		4.54	1.04	0.0114
		2.65	0.85	0.0115
50	45 / 60 mesh (0.0136)	6.40	1.08	0.0115
		4.11	0.88	0.0116
		2.13	0.45	0.0114
50	60 / 80 mesh (0.00996)	5.07	0.85	0.0115
		4.99	0.82	0.0115
		2.82	0.32	0.0114
25	45 / 60 mesh (0.0136)	3.71	0.68	0.0116
		2.58	0.40	0.0114
		1.51	0.23	0.0115

The dimensionless group, P_i, was determined to give 0.0115 for DCM, 0.0230 for DEE, and 0.0193 for DMM, whereas the corresponding intraparticle diffusion coefficients were 0.002 cm^3/sec, 0.001 cm^3/sec, and 0.0012 cm^3/sec, respectively. Results of the parameter estimation are summarized in Table 4.

Comparison of Theoretical Response to Observed Response in Time Domain

The Parameters discussed up to now can be used to predict the theoretical response curve in the time domain. For approximation, the Laplace transformed equation was inverted numerically following the curve fitting procedure suggested by Dang and Gibilaro [21].

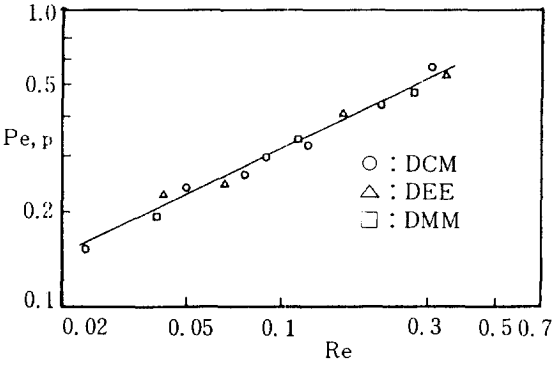

Fig. 3. Effect of Reynolds number on Peclet number for particle.

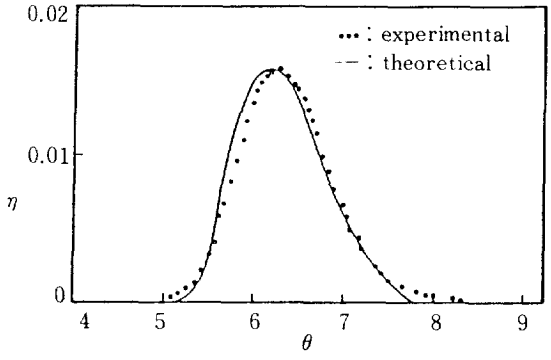

Fig. 4. Comparison of theoretical and observed response curves in time domain; DCM, (u_o=4.11cm/sec, 45/60 mesh, L=50 cm).

The infinite upper integration limit, ω_{max} was taken as the smaller value in which the amplitude ratio was 10^{-2}. Figures 4 and 5 show the theoretical response curves together with the experimental data for DCM and DMM. The agreement between the two is fairly good, but longer columns with higher flow rates often produced skewed elution curves accompanied by long tails [22].

In a chromatographic column, the mean residence time of carrier gas decreased with the increase in the flow rate. In such case, the maximum freguency was also increased because of the large amplitude ratio (Fig. 6).

The effect of Pe on the shape of the response curve was examined by comparing the experimental and theoretical responses as shown in Fig. 7. External tortuosities from I to IV were 0.1, 0.45, 0.87, and 5.0, respectively. Dotted line represents the experimental

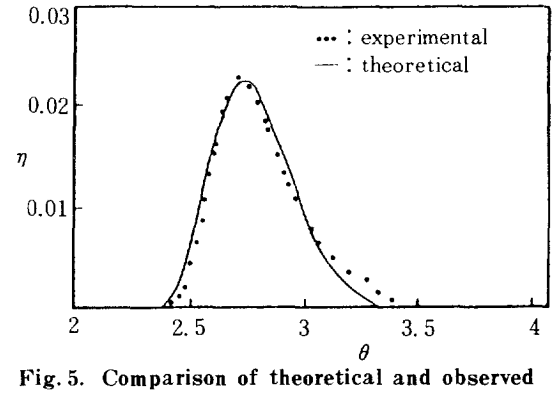

Fig. 5. Comparison of theoretical and observed response curves in time domain; DMM, other parameters as in Fig. 4.

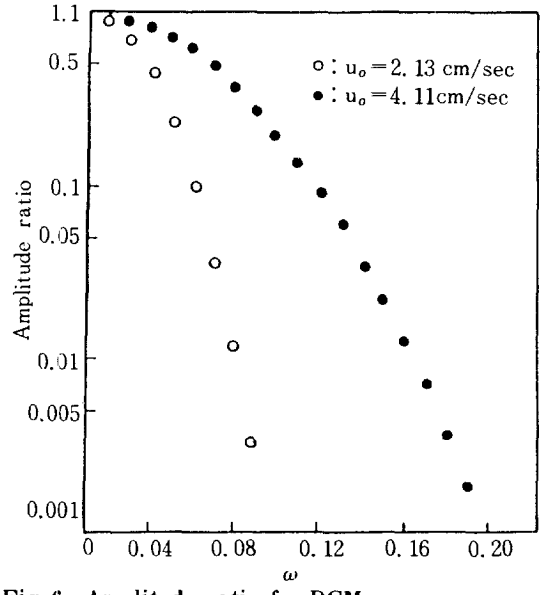

Fig. 6. Amplitude ratio for DCM,
(45/60 mesh, L=50 cm).

response curve and the corresponding tortuosity was 0.45. It is evident that, as Pe decreased, the curves became increasingly skewed. Figure 8 showsthe effect of P on the curves, and the intraparticle diffusion coefficients were 0.05, 0.001, and 0.0002 cm²/sec from the top down, while the value equivalent to the experimental curve was 0.002cm²/sec.

Sensitivity analyses of the response curves with respect to $S_t(k_f)$ and $S_tM(k_g)$ gave useful indications of how these parameters influenced the shape of the curves. The effect of the interparticle film resistance on the

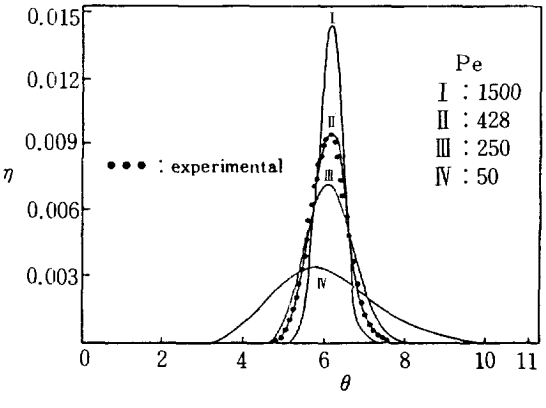

Fig. 7. Comparison of experimental and theoretical response curves showing the effect of Pe; DCM,
(u_o=2.13 cm/sec, 45/60 mesh, L=50 cm).

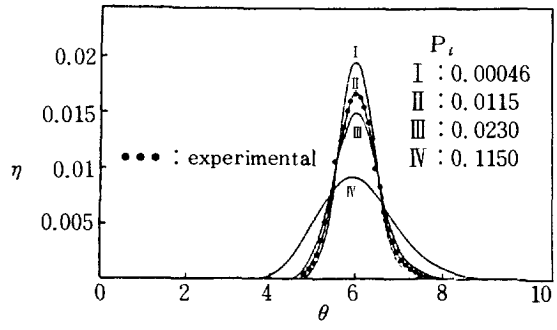

Fig. 8. Comparison of experimental and theoretical response curves showing the effect of P_t; DCM, other parameters as in Fig. 3.

response curve is illustrated in Fig. 9, from which it is found that the effect was not greatly influenced when the dimensionless group, S_t, was greater than about 1500. Curve II was obtained by using the interparticle mass transfer coefficient calculated from the equation given in Table 3.

Figure 10 shows the effect of the intraparticle film resistance on the response curve. As in Fig. 9, a decrease in the dimensionless group, S_tM, gave rise to a progressively broader peak. The theoretical response curve I was obtained by using the intraparticle mass transfer coefficient given in Table 3. The shape of the theoretical curve was not changed even though the dimensionless group. S_tM, approached to infinite. It was shown by moments analysis that the interparticle and intraparticle film resistances to the second moment of the frequency response was linearly additive [7]. So it could be concluded that the liquid film resistance was

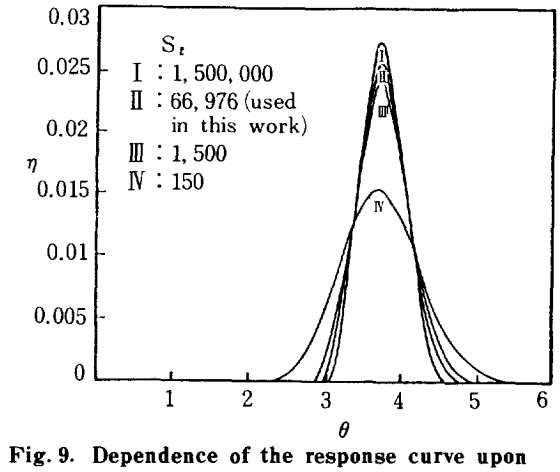

Fig. 9. Dependence of the response curve upon the interparticle mass transfer coefficient, k_f; DMM, other parameters as in Fig. 3.

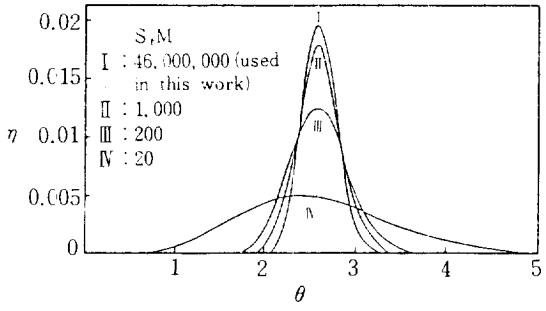

Fig. 10. Dependence of the response curve upon the intraparticle mass transfer coefficient, k_g; DEE, other parameters as in Fig. 7.

small and the diffusion in the liquid phase was not a rate-determining step.

CONCLUSIONS

With the assumption of uniform film thickness, the equations of transient material balances for the solutes were used to estimate the two parameters, η_{ext} and P_i, by the Fourier analysis, and the following results were obtained.

1. Partition coefficients for the three components (dichloromethane, diethylether, and dimethoxymethane) with dinonylphthalate-coated Chromosorb A and helium as the carrier were measured from conventional gas chromatograph. The theoretical response curves were in good agreement with the observed responses.
2. The effect of the Peclet number for particle, Pe,p, could be expressed as:
$$\frac{1}{Pe,p} = \frac{0.87}{Re \cdot Sc} - 0.5$$
3. The dimensionless groups, P_i, containing the intraparticle diffusion coefficient were 0.0115 for DCM, 0.0230 for DEE, and 0.0193 for DMM.
4. Sensitivity analyses with respect to the interparticle and intraparticle mass transfer coefficients were performed, and the result showed that the liquid film resistance was small and the diffusion in the liquid phase was not a rate-determining step.

NOMENCLATURE

A_p : surface area of porous particle per unit volume, cm^2/cm^3
A_s : surface area of porous particle per unit mass, cm^2/g
C : concentration of solute in the mobile phase, gmol/cm^3
C_l : concentration of solute in the intraparticle phase, gmol/cm^3
C_o : inlet concentration of solute, gmol/cm^3
C_s : concentration of solute in the liquid phase, gmol/cm^3
$\bar{C}(s)$: Laplace transform of C(t)
D_e : intraparticle diffusion coefficient, cm^2/sec
D_l : liquid-phase diffusion coefficient, cm^2/sec
D_M : molecular diffusivity, cm^2/sec
D_o : axial dispersion coefficient, cm^2/sec
$f_o(t), f_p(t)$: observed value and predicted value, respectively
$F_o(t), F_p(t)$: Fourier transformed transfer function
$-\Delta H_s$: heat of solution, cal/gmol
j : $\sqrt{-1}$
k_f : interparticle mass transfer coefficient, cm/sec
k_g : intraparticle mass transfer coefficient, cm/sec
K : partition coefficient
K_o : constant used in Eq. (17)
L : column length, cm
r : radial distance, cm
r_p : radius of solid support, cm
R : gas constant (1. 987 cal/gmol °K)
s : variable of Laplace transform
T : column temperature, °K
u : interstitial velocity of carrier, cm/sec
u_o : superficial velocity of carrier, cm/sec
w_L : weight of liquid phase, g
w_s : weight of solid support, g
x : distance perpendicular to surface of solid support, cm
z : axial distance. cm

Greek Letters

δ : film thickness of liquid phase, cm
ε : interparticle porosity
ε_s : intraparticle porosity with the presence of liquid phase
ε_s' : intraparticle porosity with the uncoated solid support
η_{ext} : external tortuosity
$\lambda_1, \lambda_2, \lambda_3$: values defined in Eq. (12) to Eq. (14)
μ_G : viscosity of carrier, g/cm. sec
ρ : density of carrier, g/cm^3
ρ_L : density of liquid phase, g/cm^3
ψ : objective function defined in Eq. (15)
ω, ω_{max} : frequency and maxium frequency, respectively

REFERENCES

1. King, C. J.: "Separation Processes," 2nd. Ed., McGraw Hill, N. Y. (1980).
2. Purnell, H.: "Gas Chromatography," 2nd Ed., John

Wiley & Sons,N. Y. (1967).
3. Ghim, Y. S. and Chang, H. N.: *I&EC Fundamentals,* **21,** 369 (1982).
4. Schneider, P. and Smith, J. M.: *AIChE J.,* **14,** 762 (1968).
5. Huang, S., Wilson, J. W., Wilson, D. J. and Overholser, K.A.: *J. Chromatog.,* **89,** 119 (1974).
6. Husband, W. H., Barker, P. E. and Kini, K. D.: *Transt. Instn. Chem. Engrs.,* **42,** T387 (1964).
7. Alkharasani, M. A. and McCoy, B. J.; *Chem. Eng. J.,* **23,** 81 (1982).
8. Nogare, S. D. and Juvet, R. S.: "Gas-Liquid Chromatography: Theory and Practice", John Wiley & Sons, NY (1962).
9. Chromosorb Diatomite Supports for Gas-Liquid Chromatography, Johns-Manville (1984).
10. Cadogan, D. F., Conder, J. R., Locke, D. C. and Purnell, J. H.: *J. Phys. Chem.,* **73,** 708 (1969).
11. Moon. I., Row, K.H. and Lee, W.K.: *Korean J. Chem. Eng.,* **2** (2), 155 (1985).
12. Littlewood, A. B.: "Gas Chromatography-Prinples, Techniques and Applications," Academic Press, NY (1962).
13. Giddings, J. C.: *Anal. Chem.,* **34,** 458 (1962).
14. Foo, S. C. and Rice, R. G.: *AIChE J.,* **21,** 1149 (1975).
15. Ergun, S.: *Chem. Eng. Pro.,* **48,** 227 (1952).
16. Chen, N. H. and Othmer, D. F.: *J. Chem. Eng. Data.* **7,** 37 (1962).
17. Wilke, C. R. and Chang, P.: *AIChE J.,* **1,** 264 (1955).
18. Kuester, J. L. and Mize, J. H.: "Optimization Technique with Fortran", McGraw Hill, NY (1973).
19. Wen, C. Y. and Fan, L.T.: "Models for Flow Systems and Chemical Reactors", Dekker (1975).
20. Edwards, M. F.: Ph. D. Dissertation, University of Wales (1966).
21. Dang, N. D. P. and Gibilaro, L. G.: *Chem. Eng. J.,* **8,** 157 (1974).
22. Row, K.H. and Lee, W.K.: *J. Chem. Eng. of Japan,* in press (1986).